ACS Energy LETTERS

http://pubs.acs.org/journal/aelccp

PERSPECTIVE

Toward Lead-Free Perovskite Solar Cells

Feliciano Giustino*,† and Henry J. Snaith*,‡

†Department of Materials, University of Oxford, Parks Road, Oxford OX1 3PH, U.K.

‡Department of Physics, University of Oxford, Clarendon Laboratory, Parks Road, Oxford OX1 3PU, U.K.

ABSTRACT: **Since the first reports of solar cells with power conversion efficiencies around 10% in 2012, the science and technology of perovskite photovoltaics has been progressing at an unprecedented rate. The current certified record efficiency of 22.1% makes perovskites the first solution-processable technology to outperform multicrystalline and thin-film silicon. For this technology to be deployed on a large scale, the two main challenges that need to be addressed are the material stability and the toxicity of lead. In particular, while lead is allowed in photovoltaic modules, it would be desirable to find alternatives which retain the unique optoelectronic properties of lead halide perovskites. Here we offer our perspective on the most exciting developments in the materials science of new halide perovskites, with an emphasis on alternatives to lead. After surveying recent developments of new perovskites and perovskite-related materials, we highlight the potential of halide double perovskites. This new family of compounds constitutes uncharted territory and may offer a broad materials library for solar energy applications.**

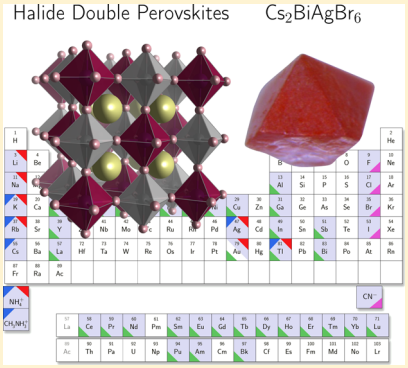

Solar cells based on halide perovskites are currently the fastest-growing photovoltaics (PV) technology in terms of research and development.[1−3] The first report on the potential of halide perovskites in PV energy conversion appeared in 2009.[4] In this study the authors employed the hybrid organic−inorganic halide perovskite $CH_3NH_3PbI_3$ as a light-sensitizer in a dye-sensitized solar cell architecture and demonstrated a power conversion efficiency (PCE) of 3.8%. The capability of halide perovskites to operate not only as strong light absorbers but also as efficient electron and hole conductors was demonstrated in two ground-breaking works in 2012,[5,6] which reported efficiencies of 10.9% and 9.7%, respectively. These works marked the beginning of a global research effort to push the performance of perovskite cells above the 20% efficiency mark, resulting in thousands of research papers published in this field during the past four years. Perovskite solar cells were soon due to break the efficiency records set by all other emerging PV technologies; at the time of writing, the highest certified efficiency is a stunning 22.1%,[7] making perovskites the first solution-processable PV technology to have surpassed the efficiency of polycrystalline and thin-film silicon solar cells. During the past four years, research on perovskite-based PV expanded toward other important optoelectronic applications, such as for example light-emitting diodes,[8] semiconductor lasers,[9] and even optical cooling by photoluminescence upconversion.[10]

The element in common to most current research on perovskite-based photovoltaics and optoelectronics is the active material, primarily a hybrid organic−inorganic perovskite based on lead, halogens, and small organic molecules. The prototypical compound of this family is methylammonium lead triiodide, $MAPbI_3$ with MA = CH_3NH_3, although in the most efficient solar cells MA is partly replaced by formamidinium, FA = $CH(NH_2)_2$.[11] $MAPbI_3$ crystallizes in the standard ABX_3 perovskite structure, as shown in Figure 1a. In this structure, Pb is at the center of regular PbI_6 octahedra, which in turn are connected in a three-dimensional corner-sharing network. The inorganic Pb−I network defines cubocthaedral cavities, each hosting one MA cation. At variance with standard perovskites, such as for example the mineral perovskite, $CaTiO_3$, where the A, B, and X elements are in their formal oxidation states +2, + 4, and −2, respectively, in halide perovskites one finds the formal charges $CH_3NH_3^+$, Pb^{2+}, and I^-. At low temperature, $MAPbI_3$ crystallizes in a orthorhombic lattice with space group *Pnma*,[12,13] see Figure 1a. With increasing temperature the system undergoes a first phase transition to a tetragonal lattice with space group *I4/mcm* at 165 K and then becomes (pseudo)cubic at 327 K with space group $Pm\bar{3}m$. The topology of the perovskite structure is retained across these phase transitions; in fact, the structural changes are associated with a progressive suppression of octahedral tilts and the thermal activation of the spinning and tumbling of the MA cations.[12−14]

$MAPbI_3$ exhibits a number of remarkable properties that make it ideal for optoelectronics applications. It is a direct-gap semiconductor, with a band gap of 1.6 eV at room temperature,[15] very near the optimal Schockley−Queisser gap for single-junction solar cells (1.43 eV). It is a strong light

Received: October 3, 2016
Accepted: November 14, 2016
Published: November 14, 2016

DOI: 10.1021/acsenergylett.6b00499
ACS Energy Lett. 2016, 1, 1233−1240

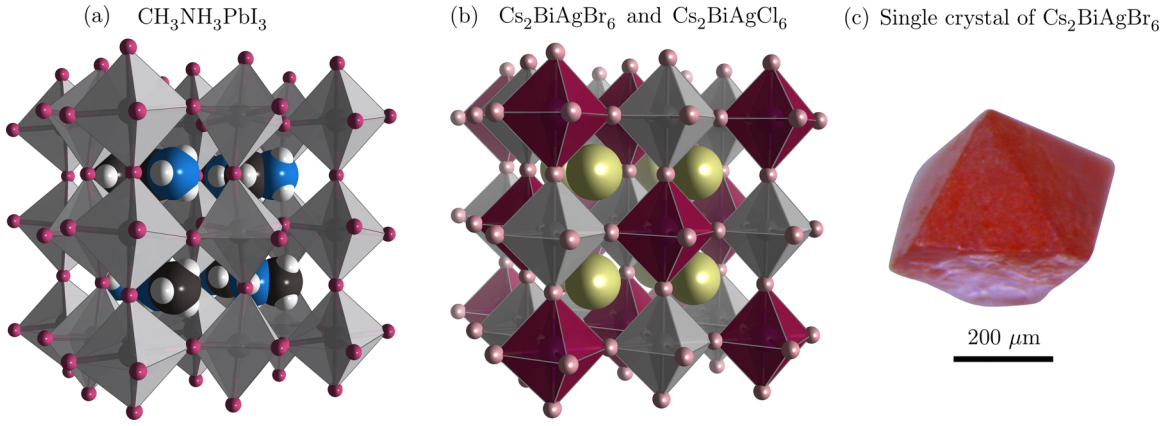

Figure 1. (a) Polyhedral model of $MAPbI_3$ in the low-temperature orthorhombic phase. PbI_6 octahedra are in gray; the I anions are brown; and the large spheres in the cavities represent the $CH_3NH_3^+$ cations (N is blue, C is black). (b) Polyhedral model of $Cs_2BiAgBr_6$ in the room-temperature cubic phase. Cs is in yellow, and Br is pink; the $BiBr_6$ and $AgBr_6$ octahedra are in dark red and gray, respectively. (c) Photograph of a single crystal of $Cs_2BiAgBr_6$ (courtesy of A. A. Haghighirad, University of Oxford).

absorber, with an absorption coefficient $\alpha = 5 \times 10^4$ cm^{-1} in the red (1.7 eV), about 25 times higher than that in silicon and even superior to that of GaAs.[16] The absorption onset is extremely sharp, with an Urbach energy as small as 13 meV and comparable (though slightly higher) to that of GaAs.[16−18] The photogenerated electrons and holes are long-lived[19] and exhibit diffusion lengths as long as 1 μm.[20−22] In addition, the electron and hole effective masses are small and balanced,[23] leading to efficient ambipolar transport. These properties also enable photon recycling in $MAPbI_3$,[24] that is, the dissipationless absorption and emission of photons within the sample. This effect leads to an optimal utilization of solar photons within the active layer. Given their outstanding properties, $MAPbI_3$ and related compounds can be considered as the "first high-quality halide semiconductors".[25] The unique optoelectronic properties of lead halide perovskites are even more surprising when considering that these films are routinely prepared by inexpensive solution-processing routes. The ease of fabrication makes halide perovskites ideally suited for scaling up the production using ink-based printing or spray-coating techniques.

The perovskite structure naturally lends itself to combinatorial chemistry. Following the development of solar cells based on $MAPbI_3$, many studies focused on the optimization of the materials by testing alternatives for the organic and metal cations as well as for the halides.[11,26,27] Successful examples of materials optimization include solar cells based on solid solutions of $FAPbI_3$ and $MAPbBr_3$,[28] mixes of FA/Cs and I/Br,[29] triple-cation configurations such as Cs/MA/FA,[30] and perovskite−perovskite tandem devices employing Sn/Pb mixes.[31] Interestingly, only $MAPbI_3$ forms a stable perovskite phase at room temperature, although mixtures of FA and Cs, Cs and MA, or MA and FA also yield crystal phases that are stable at room temperature. By tuning the compositions in the solid solutions it is therefore possible to identify "sweet spots" with good stability and high PV efficiency.

As current research on perovskite photovoltaics is rapidly approaching the theoretical efficiency limit for single junction solar cells, it is natural to ask what stands between the research in the laboratories and the deployment of this technology on a large scale. It is clear by now that the main outstanding issue is the tendency of these materials to degrade under exposure to moisture, heating, or prolonged illumination in air.[32] This issue has partly been addressed via compositional engineering;[28−30] however, it still remains to be seen whether it will be possible to extend the lifespan of perovskite solar cells from several weeks to several tens of years. The second possible issue is the presence of Pb in the perovskite crystal. This does not pose a problem if Pb remains contained within the PV module; however, lead-based perovskites tend to release PbI_2 as a degradation product, which is toxic. Human exposure to lead is harmful to the nervous and reproductive systems and to the hematopoietic and renal organs, mainly as a result of increased oxidative stress.[33]

One viable option for reducing the hazards of Pb exposure is to develop effective encapsulation strategies. In order for commercial solar panels to last for more than 25 years, the modules have to be extremely well encapsulated against moisture and oxygen ingress. In the most robust encapsulation protocols this is typically achieved by laminating the modules between two sheets of glass and polymer foil, followed by careful edge sealing. Furthermore, at the end of the module lifetime, it is important to ensure that all materials be recycled, as already happens for commercial thin-film PV technologies such as CdTe and CIGS. In practice, Pb is allowed in PV modules because solar panels are exempted from legislation such as the European Restriction on Hazardous Substances (RoHS).[3] This exemption enables the continued use of existing PV modules, which also contain a significant amount of Pb.

> Pb is allowed in PV modules, but it would be preferable to find an alternative.

In addition to improving the encapsulation of perovskites, another option is to replace Pb altogether in these materials. Alternatives to lead must fulfill very stringent criteria in order to match the performance of lead-halide perovskites. For example, the new compounds must exhibit excellent optoelectronics properties, comparable to the best inorganic semiconductors such as GaAs;[25] this requires direct band gaps for strong light absorption and photon recycling, as well as very small and balanced effective masses for efficient ambipolar transport. Furthermore, the new compounds should be defect-tolerant as is the case for $MAPbI_3$,[34] so as to suppress nonradiative

DOI: 10.1021/acsenergylett.6b00499
ACS Energy Lett. 2016, 1, 1233−1240

recombination channels. Finally, the new compounds should ideally be processable from solution in order to be competitive with established PV technologies. Taken together, these requirements render the elimination of Pb from perovskite solar cells a formidable scientific challenge.

The most obvious choice for Pb replacement is to use another group 14 metal, such as Sn or Ge. This would be a natural development, especially because the very first organic–inorganic halide perovskites used in optoelectronic devices were based on Sn.[35] From a fundamental standpoint, Sn-based halide perovskites constitute very promising materials for optoelectronic applications, owing to their optical band gaps in the red/infrared and good charge-carrier mobilities.[26] In 2012, the Sn-based perovskite $CsSnI_3$ was successfully employed as the inorganic hole-transporter in solid-state dye-sensitized solar cells.[36] In 2014, solar cells based entirely on the organic–inorganic Sn halide perovskites $CH_3NH_3SnI_3$[37] and $CH_3NH_3Sn(I_{1-x}Br_x)_3$[38] were demonstrated, with energy conversion efficiencies of 6.4% and 5.73%, respectively. Despite their proven potential, Sn-based perovskites are prone to self-doping effects and structural instabilities, owing to the known tendency of Sn^{2+} to oxidize into Sn^{4+}; as a result, organic–inorganic perovskites based on Sn tend to degrade rapidly upon exposure to ambient air, and the device fabrication requires processing in nitrogen-filled glove-boxes.[37,38] Furthermore, it is unclear whether Sn would be a safer alternative to Pb, because one of the degradation products, SnI_2, may be as harmful as its lead counterpart PbI_2.[39] Recent progress in this direction includes the stabilization of Sn in mixed Sn/Pb perovskites such as $FA_{0.75}Cs_{0.25}Sn_{0.5}Pb_{0.5}I_3$.[31]

These considerations raise a fundamental question: is it possible to completely replace Pb in perovskites solar cells by nontoxic elements, without compromising efficiency and stability, or is it the case that Pb is absolutely essential? In an attempt to answer this question, two recent computational studies screened all possible hypothetical halide perovskites that can be generated via homovalent replacement of Pb.[40,41] In ref 40, the authors investigated the electronic structure of hypothetical $CsB^{2+}X_3$ perovskites with X = Cl, Br, I using the low-temperature orthorhombic phase of $CH_3NH_3PbI_3$ as a starting template. For the metal cations B^{2+}, the authors considered all possible elements which form dihalide salts, yielding more than a hundred unique compounds. This study revealed that no other metal cation is able to match the unique optoelectronic properties of Pb- and Sn-based perovskites, such as direct band gaps in the visible and low electron and hole effective masses. In ref 41, the authors performed a high-throughput search for stable ABX_3 perovskites using the high-temperature cubic structure as a starting template. Even after considering more than 32 000 hypothetical perovskites, the authors found that the only halide perovskites showing promise for PV applications were precisely compounds based on Pb, Sn, or Ge. Both these studies support the notion that halide perovskites based on Pb or Sn are truly unique in terms of optoelectronic properties.

In an attempt to stabilize Sn-based perovskites, several groups reported Sn-based halide perovskite derivatives with general composition A_2SnX_6, for example Cs_2SnI_6,[42,43] $Cs_2Sn(I,Br)_6$,[44] and Cs_2SnX_6 with X = Cl, Br, I.[45] These compounds exhibit good stability in air and moisture, due to the presence of Sn in its stable +4 oxidation state. The crystal structures can be thought of as being derived from the cubic double perovskites $Cs_2Sn_2X_6$ by removing half of the octahedral Sn atoms, so as to obtain a molecular salt formed by Cs^+ cations and $[SnI_6]^{2-}$ octahedra as anions, as shown in Figure 2. Because the Sn

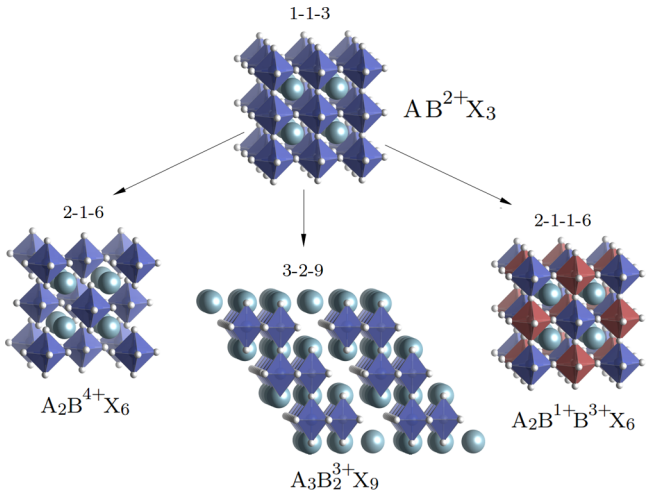

Figure 2. Schematic relation between the crystal structures of Pb-perovskites and lead-free perovskite derivatives. Moving from left to right, 2−1−6 compounds like Cs_2SnI_6 can be thought of as if obtained from lead halide perovskites by removing half of the B-site cations in a checkerboard pattern. In this case, charge neutrality requires the B-site cation to be in its +4 oxidation state. 3−2−9 compounds like $Cs_3Sb_2I_9$ can be imagined as derived from the perovskite at the top by removing one B-site cation every three, with all cations removed from planes defined by the ⟨111⟩ directions of the cubic perovskite crystal. In this case, the B-site cation must be in the +3 oxidation state in order to maintain charge neutrality. When the ionic radius of the A-site cation is large, the structure of these 3−2−9 compounds transforms into isolated face-sharing bioctahedra, as in $MA_3Sb_2I_9$. 2−1−1−6 compounds like $Cs_2BiAgCl_6$ can be thought of as if obtained from the perovskite at the top by replacing every pair of adjacent B^{2+} cations by one B^{1+} and one B^{3+} cation, so as to define a rock-salt arrangement of cations.

vacancies define a regular sublattice of the double perovskite structure, these compounds are termed "vacancy ordered" double perovskites, and indicated as $Cs_2Sn^{4+}\square I_6$ ($\square$ stands for vacancy).[43] One intriguing feature of these materials is that, while they are reminiscent of molecular crystals, they exhibit unusually dispersive electronic band structures and direct band gaps which can be as low as 1.3 eV in the case of Cs_2SnI_6.[45]

The concept of vacancy-ordered perovskites can also be used to describe new compounds with formula unit $A_3B_2X_9$, where A is a monovalent cation and B is a trivalent metal cation.[46−49] These compounds can be thought of as perovskites of composition $AB_{2/3}X_3$, where one in three octahedral B^{3+} sites is vacant in order to maintain charge neutrality. The resulting structures are termed "two-dimensional layered perovskite derivatives" and crystallize in the $P\bar{3}m1$ space group (Figure 2). In these compounds, Pb^{2+} is replaced by Sb^{3+} or Bi^{3+}, e.g., as in $Cs_3Sb_2I_9$[46] and $Rb_3Sb_2I_9$.[50] For large A-site cations these structures can transform into zero-dimensional dimers of face-sharing BX_6 octahedra (space group $P6_3/mmc$), for example, as in $MA_3Sb_2I_9$[48] and $MA_3Bi_2I_9$.[47] All these compounds have band gaps around 2.1 eV and exhibit enhanced air stability as compared to $MAPbI_3$. Mesoscopic heterojunction solar cells were reported for $Cs_3Bi_2I_9$ (1.09% PCE),[47] $Rb_3Sb_2I_9$ (0.66% PCE),[50] and $MA_3Bi_2I_9$ (0.2% PCE);[49] while planar heterojunction devices were reported for $MA_3Sb_2I_9$ (0.5% PCE).[48]

DOI: 10.1021/acsenergylett.6b00499
ACS Energy Lett. 2016, 1, 1233−1240

Table 1. Summary of Pb-Free Perovskites and Perovskite Derivatives[a]

family	stoichiom.	compound	solut.	solid st.	gap (eV)	PCE (%)	ref
perovskite	1−1−3	$MASnI_3$	×	×	1.20−1.35		26
		$MASnI_3$	×		1.23	6.4	37
		$MASn_{1-x}Pb_xI_3$[b]	×	×	1.21−1.54		26
		$MASnI_{3-x}Br_x$		×	1.30−2.15	5.73	38
		$FASnI_3$	×	×	1.41		26
		$CsSnI_3$	×	×	1.30		26
vacancy-ordered	2−1−6	Cs_2SnI_6	×		1.26	6.94[c]	42
double perovskite		Cs_2SnBr_6	×		2.7	0.04[c]	45
		Cs_2SnCl_6	×		3.9	0.07[c]	45
		$Cs_2Sn_{1-x}Te_xI_6$[d]	×		1.25−1.59		43
two-dimensional	3−2−9	$Cs_3Sb_2I_9$		×[e]	2.05		46
perovskite		$Cs_3Bi_2I_9$	×		2.2	1.09	47
		$MA_3Sb_2I_9$	×		2.14	0.5	48
		$MA_3Bi_2I_9$	×		2.1	0.12	47
		$MA_3Bi_2I_9$	×			0.2	49
		$Rb_3Sb_2I_9$	×		2.1−2.24	0.66	50
double perovskite	2−1−1−6	$Cs_2BiAgBr_6$		×	1.95		54
(elpasolite)		$Cs_2BiAgBr_6$	×	×	2.19		55
		$Cs_2BiAgBr_6$	×	×	1.9		58
		$Cs_2BiAgCl_6$	×	×	2.77		55
		$Cs_2BiAgCl_6$		×	2.2		56
		MA_2BiKCl_6	×		3.04		57
(other)	1−2−7	$AgBi_2I_7$	×		1.87	1.22	51
(other)	1−1−5	$HDABiI_5$	×		2.1	0.027	53

[a]We indicate the family name, stoichiometry, chemical formula, synthetic method (from solution or solid-state synthesis), measured band gap, and power-conversion efficiency for those cases where devices have been reported. [b]x = 0, 0.25, 0.50, 0.75, 1. [c]Used as a hole transporter in a dye-sensitized cell. [d]x = 0, 0.1, 0.25, 0.5, 0.75, 0.9, 1. [e]Fabricated through evaporation.

Related lead-free compounds include $AgBi_2I_7$,[51,52] for which solar cells with PCE of 1.22% were reported,[51] and $HDABiI_5$, where HDA is the divalent organic cation 1,6-hex-anediammonium.[53] Table 1 summarizes these recently reported lead-free perovskites and perovskites derivatives, together with the corresponding device efficiencies where available.

An alternative possibility to realize lead-free compounds retaining the conventional perovskite structure but without resorting to Sn is to explore heterovalent substitution of Pb^{2+} by pairs of B-site cations with formal oxidation states +1 and +3 (Figure 2). This possibility was recently investigated in four independent studies.[54−57] These studies reported on the synthesis of novel "double perovskites" based on bismuth and monovalent metals. In particular, ref 56 reported the computational screening of the hypothetical perovskites $Cs_2BB^{3+}X_6$, with B^{3+} = Bi, Sb; B = Cu, Ag, Au; X = Cl, Br, I. Many of these hypothetical compounds were predicted to exhibit promising optoelectronic properties, such as band gaps in the visible and low effective masses. The authors of this study also reported the synthesis and characterization of the new double perovskite $Cs_2BiAgCl_6$. In ref 54, the authors reported the synthesis and characterization of the related compound $Cs_2BiAgBr_6$, and ref 55 reported both $Cs_2BiAgCl_6$ and $Cs_2BiAgBr_6$. The first step toward Pb-free hybrid organic−inorganic double perovskites was demonstrated in ref 57, with the synthesis of $(CH_3NH_3)_2KBiCl_6$.

According to these initial investigations, the new halide double perovskites have indirect band gaps ranging from 1.8−2.2 eV ($Cs_2BiAgBr_6$)[54,55,58] to 2.2−2.8 eV ($Cs_2BiAgCl_6$),[55,56,58] exhibit strong luminesce in the visible, and have long recombination lifetimes (660 ns, ref 54). First-principles calculations indicate that the bottom of the conduction band is predominantly of antibonding Bi-6p/halogen-p character, while the top of the valence band is associated with Ag-4d/halogen-p antibonding orbitals.[58] The effective masses calculated in ref 56 are relatively anisotropic, with the lightest electron masses comparable to those of $CH_3NH_3PbI_3$. Both $Cs_2BiAgBr_6$ and $Cs_2BiAgCl_6$ appear considerably more stable than Pb-based perovskites in ambient air. For example, the X-ray diffraction pattern of $Cs_2BiAgCl_6$ does not show any noticeable changes after 3 weeks in ambient air;[56] furthermore, degradation in $Cs_2BiAgBr_6$ is observed only upon light exposure for 2 weeks.[55]

Pb-free double perovskites will be a promising new research direction in perovskite PV and halide-based optoelectronics.

The structure of $Cs_2BiAgBr_6$ is shown in Figure 1b. At room temperature, this compound crystallizes in a face-centered cubic structure with space group $Fm\bar{3}m$. The Bi and Ag cations alternate along the [100], [010], and [001] directions, so that the BiAg sublattice defines a rock-salt structure as in NaCl. This compound can be understood as a cubic perovskite with a doubled unit cell, that is, a "double perovskite". $Bi^{3+}Ag^{1+}$ double perovskites were obtained either by solution processing or via solid-state reaction,[54−56,58] with the samples prepared from solution exhibiting higher phase purity.[55] The solution-based synthesis involves moderate temperatures (<150 °C) and yields a polycrystalline material upon cooling to room temperature. The resulting compound consists of octahedron-shaped crystals with sizes ranging from 0.1 mm[56] to 4 mm,[54] depending on the

DOI: 10.1021/acsenergylett.6b00499
ACS Energy Lett. 2016, 1, 1233−1240

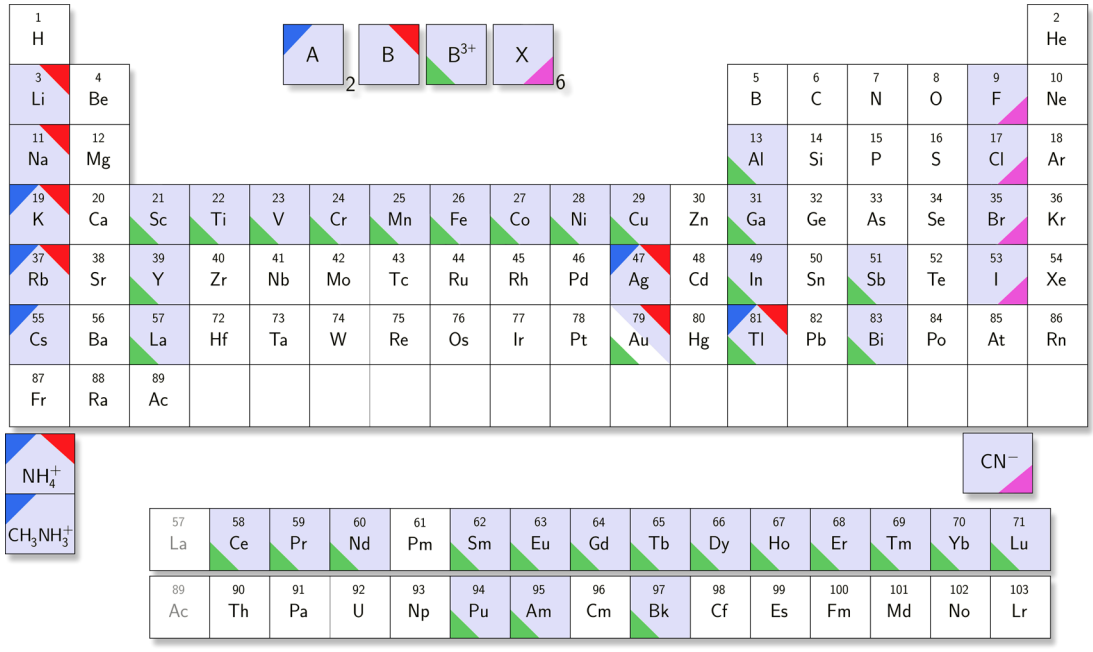

Figure 3. Elements forming halide double perovskites (elpasolites) with composition $A_2BB^{3+}X_6$. An element is colored in light blue if at least one compound with elpasolite structure containing that element has been synthesized. The triangular color tag specifies the site occupied by the element, according to the legend at the top. The compounds used to generate the table are described in refs 57 and 59−74. Only structures that crystallize in the space group *Fm*3*m* at room temperature have been considered for this table. The element Au is half-colored because it exists only in the compounds $A_2Au_2X_6$ with A = Rb, Cs and X = Cl, Br, I. The structure of these compounds is obtained from the standard double perovskite by alternating compressed and elongated AuX_6 octahedra.[75]

cooling rate. Figure 1c shows a photograph of a small single crystal of $Cs_2BiAgBr_6$, with its characteristic dark red color indicating a band gap in the visible.

While Pb-free double perovskites are only making their debut in solar energy research, related compounds have been known for many years under the name of "elpasolites". Elpasolite is the name of the mineral K_2NaAlF_6, first discovered in El Paso County, Colorado. Nowadays, synthetic elpasolites find applications as scintillators for the detection of γ-rays, X-rays, and neutrons. For example, the most-studied elpasolite scintillator is $Cs_2LiYCl_6:Ce^{3+}$, that is, a Cs_2LiYCl_6 elpasolite crystal doped with Ce^{3+} impurities (typically 0.1%) on the B^{3+} = Y site. This system has a very wide band gap (>6 eV), and the Ce^{3+} 4f and 5d states are located within the gap. Electrons and holes generated by ionizing radiation can form self-trapped excitons at the impurity sites, and the material scintillates upon radiative recombination.[76] This compound is also employed in the detection of thermal neutrons, by exploiting the high neutron absorption cross section of ^{6}Li and the reaction $^6Li(n,\alpha)$.

A survey of the literature on elpasolites shows that these compounds offer immense opportunities in terms of combinatorial chemistry. Already in 1982, for example, 234 cubic or tetragonal halide elpasolites structures were known.[77] A more recent review suggests that at least 350 different elpasolites have been synthesized.[78] In Figure 3 we highlight all the elements of the periodic table which belong to known halide elpasolites.[57,59−74] A simple count indicates that 7 elements are found as A-site cations, 8 elements can occupy the B^+ sites (including ammonium and methylammonium), 34 elements are found as B^{3+} cations, and 5 elements can occupy the X sites (including the cyanide CN^-). A straightforward multiplication of these numbers yields a stunning 9520 combinations. Following Goldschmidt's rules,[79] we must expect that the majority of these combinations will correspond to unstable compounds; however, even within the pessimistic scenario that only 10% of these 9520 combinations are amenable to synthesis, we would still be facing over 900 possible compounds, out of which more than 600 compounds have never hitherto been investigated. These simple considerations suggest that the new halide double perovskites $Cs_2BiAgCl_6$, $Cs_2BiAgBr_6$, and $(CH_3NH_3)_2KBiCl_6$ may be only the tip of the iceberg, and that an entire new family of semiconductors may be waiting to be discovered. The computational screening of more than 600 hypothetical halide double perovskites represents a demanding task, but it certainly is within the reach of today's computational capabilities.[80] This suggests that ab initio computations are ideally positioned to spearhead the search for new semiconducting perovskites.

> Ab initio computations are ideally positioned to spearhead the search for new semiconducting perovskites.

Much work remains to be done in order to assess the potential of lead-free halide perovskites. For example, working solar cells based on $Cs_2BiAgBr_6$ have not been reported to date. This is largely due to the difficulty in developing a synthetic route to obtain uniform thin films of the correct phase and composition. The development of effective synthesis methods constitutes a priority for current and future research in this area. Another important limitation of the recently reported halide double perovskites is their indirect band gap. If lead-free materials are to match the unparalleled performance of their Pb-based counterparts, it will be important to devise strategies

DOI: 10.1021/acsenergylett.6b00499
ACS Energy Lett. 2016, 1, 1233−1240

in order to engineer a direct band gap with a strong oscillator strength for optical transitions. Finally, it will be critical to see how these new compounds and related low-gap double perovskites will perform in a solar cell under standard operating conditions.

These and many other challenges will have to be addressed before these new materials become competitive alternatives, but with some optimism we anticipate that double perovskites will be a promising new research direction in perovskite PV and halide-based optoelectronics. Could it be that the road toward safe and environmentally friendly solar energy eventually leads to El Paso?

AUTHOR INFORMATION

Corresponding Authors

*E-mail: feliciano.giustino@materials.ox.ac.uk. Phone: (+44) 1865 612790.

*E-mail: henry.snaith@physics.ox.ac.uk. Phone: (+44) 1865 272380.

ORCID

Feliciano Giustino: 0000-0001-9293-1176

Notes

The authors declare no competing financial interest.

Biographies

Feliciano Giustino is Professor of Materials at the University of Oxford. His research is focused on the atomic-scale design of advanced functional materials and ab initio electronic structure methods.

Henry J. Snaith is Professor of Physics at the University of Oxford. His research is focused on organic and hybrid optoelectronic materials and devices, and specifically on perovskite solar cells.

ACKNOWLEDGMENTS

This work was supported by the Leverhulme Trust (Grant RL-2012-001), the UK Engineering and Physical Sciences Research Council (grants No. EP/J009857/1 and EP/M020517/1), and the European Union's Horizon 2020 research and innovation programme under grant agreement No. 696656 - GrapheneCore1.

REFERENCES

(1) Green, M. A.; Bein, T. Photovoltaics: Perovskite Cells Charge Forward. *Nat. Mater.* **2015**, *14*, 559−561.

(2) Stranks, S.; Snaith, H. J. Metal-halide Perovskites for Photovoltaic and Light-Emitting Devices. *Nat. Nanotechnol.* **2015**, *10*, 391−402.

(3) Green, M. A.; Ho-Baillie, A.; Snaith, H. J. The Emergence of Perovskite Solar Cells. *Nat. Photonics* **2014**, *8*, 506−514.

(4) Kojima, A.; Teshima, K.; Shirai, Y.; Miyasaka, T. Organometal Halide Perovskites as Visible-Light Sensitizers for Photovoltaic Cells. *J. Am. Chem. Soc.* **2009**, *131*, 6050−6051.

(5) Lee, M. M.; Teuscher, J.; Miyasaka, T.; Murakami, T. N.; Snaith, H. J. Efficient Hybrid Solar Cells Based on Meso-Superstructured Organometal Halide Perovskites. *Science* **2012**, *338*, 643−647.

(6) Kim, H.-S.; Lee, C. R.; Im, J.-H.; Lee, K.-B.; Moehl, T.; Marchioro, A.; Moon, S.-J.; Humphry-Baker, R.; Yum, J.-H.; Moser, J. E.; et al. Lead Iodide Perovskite Sensitized All-Solid-State Submicron Thin Film Mesoscopic Solar Cell with Efficiency Exceeding 9%. *Sci. Rep.* **2012**, *2*, 591.

(7) Green, M. A.; Emery, K.; Hishikawa, Y.; Warta, W.; Dunlop, E. D. Solar Cell Efficiency Tables (Version 48). *Prog. Photovoltaics* **2016**, *24*, 905−913.

(8) Tan, Z.-K.; Moghaddam, R. S.; Lai, M. L.; Docampo, P.; Higler, R.; Deschler, F.; Price, M.; Sadhanala, A.; Pazos, L. M.; Credgington, D.; et al. Bright Light-Emitting Diodes Based on Organometal Halide Perovskite. *Nat. Nanotechnol.* **2014**, *9*, 687−692.

(9) Zhu, H.; Fu, Y.; Meng, F.; Wu, X.; Gong, Z.; Ding, Q.; Gustafsson, M. V.; Trinh, M. T.; Jin, S.; Zhu, X. Lead Halide Perovskite Nanowire Lasers With Low Lasing Thresholds and High Quality Factors. *Nat. Mater.* **2015**, *14*, 636−642.

(10) Ha, S.-T.; Shen, C.; Zhang, J.; Xiong, Q. Laser Cooling of Organic-Inorganic Lead Halide Perovskites. *Nat. Photonics* **2015**, *10*, 115−121.

(11) Eperon, G. E.; Stranks, S. D.; Menelaou, C.; Johnston, M.; Herz, L. M.; Snaith, H. J. Formamidinium Lead Trihalide: Broadly Tunable Perovskite Heterojunction Solar Cells. *Energy Environ. Sci.* **2014**, *7*, 982−988.

(12) Baikie, T.; Fang, Y.; Kadro, J. M.; Schreyer, M.; Wei, F.; Mhaisalkar, S. G.; Grätzel, M.; White, T. J. Synthesis and Crystal Chemistry of the Hybrid Perovskite ($CH_3NH_3PbI_3$) for Solid-State Sensitized Solar Applications. *J. Mater. Chem. A* **2013**, *1*, 5628−5641.

(13) Weller, M. T.; Weber, O. J.; Henry, P. F.; Di Pumpo, A. M.; Hansen, T. C. Complete Structure and Cation Orientation in the Perovskite Photovoltaic Methylammonium Lead Iodide Between 100 and 352 K. *Chem. Commun.* **2015**, *51*, 4180−4183.

(14) Leguy, A. M.; Frost, J. M.; McMahon, A. P.; Sakai, V. G.; Kochelmann, W.; Law, C.; Li, X.; Foglia, F.; Walsh, A.; O'regan, B. C.; et al. The Dynamics of Methylammonium Ions in Hybrid Organic-Inorganic Perovskite Solar Cells. *Nat. Commun.* **2015**, *6*, 7124.

(15) D'Innocenzo, V.; Grancini, G.; Alcocer, M. J. P.; Kandada, A. R. S.; Stranks, S. D.; Lee, M. M.; Lanzani, G.; Snaith, H. J.; Petrozza, A. Excitons Versus Free Charges in Organo-Lead Tri-Halide Perovskites. *Nat. Commun.* **2014**, *5*, 3586.

(16) De Wolf, S.; Holovsky, J.; Moon, S.-J.; Löper, P.; Niesen, B.; Ledinsky, M.; Haug, F.-J.; Yum, J.-H.; Ballif, C. Organometallic Halide Perovskites: Sharp Optical Absorption Edge and its Relation to Photovoltaic Performance. *J. Phys. Chem. Lett.* **2014**, *5*, 1035−1039.

(17) Sadhanala, A.; Deschler, F.; Thomas, T. H.; Dutton, S. E.; Goedel, K. C.; Hanusch, F. C.; Lai, M. L.; Steiner, U.; Bein, T.; Docampo, P.; et al. Preparation of Single-Phase Films of $CH_3NH_3Pb(I_{1-x}Br_x)_3$ with Sharp Optical Band Edges. *J. Phys. Chem. Lett.* **2014**, *5*, 2501−2505.

(18) Sadhanala, A.; Kumar, A.; Pathak, S.; Rao, A.; Steiner, U.; Greenham, N. C.; Snaith, H. J.; Friend, R. H. Electroluminescence from Organometallic Lead Halide Perovskite-Conjugated Polymer Diodes. *Adv. Electron. Mater.* **2015**, *1*, 1500008.

(19) Wehrenfennig, C.; Eperon, G. E.; Johnston, M. B.; Snaith, H. J.; Herz, L. M. High Charge Carrier Mobilities and Lifetimes in Organolead Trihalide Perovskites. *Adv. Mater.* **2014**, *26*, 1584−1589.

(20) Stranks, S. D.; Grancini, G. E.; Menelaou, G.; Alcocer, C.; Leijtens, M. J. P.; Herz, L. M.; Petrozza, A.; Snaith, H. J. Electron-Hole Diffusion Length Exceeding 1 Micrometer in an Organometal Trihalide Perovskite Absorber. *Science* **2013**, *342*, 341−344.

(21) Xing, G.; Mathews, N.; Sun, S.; Lim, S. S.; Lam, Y. M.; Grätzel, M.; Mhaisalkar, S.; Sum, T. C. Long Range Balanced Electron- and Hole-Transport Lengths in Organic-Inorganic $CH_3NH_3PbI_3$. *Science* **2013**, *342*, 344−347.

(22) Dong, Q.; Fang, Y.; Shao, Y.; Mulligan, P.; Qiu, J.; Cao, L.; Huang, J. Electron-Hole Diffusion Lengths > 175μm in Solution Grown $CH_3NH_3PbI_3$ Single Crystals. *Science* **2015**, *347*, 967−970.

(23) Miyata, A.; Mitioglu, A.; Plochocka, P.; Portugall, O.; Wang, J. T.-W.; Stranks, S. D.; Snaith, H. J.; Nicholas, R. J. Direct Measurement of the Exciton Binding Energy and Effective Masses for Charge Carriers in an Organic-Inorganic Tri-Halide Perovskite. *Nat. Phys.* **2015**, *11*, 582−587.

(24) Pazos-Outón, L. M.; Szumilo, M.; Lamboll, R.; Richter, J. M.; Crespo-Quesada, M.; Abdi-Jalebi, M.; Beeson, H. J.; Vrućinić, M.; Alsari, M.; Snaith, H. J.; et al. Photon Recycling in Lead Iodide Perovskite Solar Cells. *Science* **2016**, *351*, 1430−1433.

(25) Yablonovitch, E. Lead Halides Join the Top Optoelectronic League. *Science* **2016**, *351*, 1401−1401.

(26) Stoumpos, C. C.; Malliakas, C. D.; Kanatzidis, M. G. Semiconducting Tin and Lead Iodide Perovskites with Organic

DOI: 10.1021/acsenergylett.6b00499
ACS Energy Lett. 2016, 1, 1233−1240

Cations: Phase Transitions, High Mobilities, and Near-Infrared Photoluminescent Properties. *Inorg. Chem.* **2013**, *52*, 9019−9038.
(27) Filip, M. R.; Eperon, G.; Snaith, H. J.; Giustino, F. Steric Engineering of Metal-Halide Perovskites with Tunable Optical Band Gaps. *Nat. Commun.* **2014**, *5*, 5757.
(28) Jeon, N. J.; Noh, J. H.; Yang, W. S.; Kim, Y. C.; Ryu, S.; Seo, J.; Seok, S. I. Compositional Engineering of Perovskite Materials for High-Performance Solar Cells. *Nature* **2015**, *517*, 476−480.
(29) McMeekin, D. P.; Sadoughi, G.; Rehman, W.; Eperon, G. E.; Saliba, M.; Hörantner, M. T.; Haghighirad, A.; Sakai, N.; Korte, L.; Rech, B.; et al. A Mixed-Cation Lead Mixed-Halide Perovskite Absorber for Tandem Solar Cells. *Science* **2016**, *351*, 151−155.
(30) Saliba, M.; Matsui, T.; Seo, J.-Y.; Domanski, K.; Correa-Baena, J.-P.; Nazeeruddin, M. K.; Zakeeruddin, S. M.; Tress, W.; Abate, A.; Hagfeldt, A.; et al. Cesium-Containing Triple Cation Perovskite Solar Cells: Improved Stability, Reproducibility and High Efficiency. *Energy Environ. Sci.* **2016**, *9*, 1989−1997.
(31) Eperon, G. E.; Leijtens, T.; Bush, K. A.; Green, T.; Tse-Wei Wang, J.; McMeekin, D. P.; Volonakis, G.; Milot, R. L.; Slotcavage, D. J.; Belisle, R.; et al. Perovskite-Perovskite Tandem Photovoltaics with Ideal Bandgaps. *Science* **2016**, DOI: 10.1126/science.aaf9717.
(32) Berhe, T. A.; Su, W.-N.; Chen, C.-H.; Pan, C.-J.; Cheng, J.-H.; Chen, H.-M.; Tsai, M.-C.; Chen, L.-Y.; Dubale, A. A.; Hwang, B.-J. Organometal Halide Perovskite Solar Cells: Degradation and Stability. *Energy Environ. Sci.* **2016**, *9*, 323−356.
(33) Flora, G.; Gupta, D.; Tiwari, A. Toxicity of Lead: a Review with Recent Updates. *Interdiscip. Toxicol.* **2012**, *5*, 47−58.
(34) Brandt, R. E.; Stevanović, V.; Ginley, D. S.; Buonassisi, T. Identifying Defect-Tolerant Semiconductors with High Minority-Carrier Lifetimes: Beyond Hybrid Lead Halide Perovskites. *MRS Commun.* **2015**, *5*, 265−275.
(35) Kagan, C. R.; Mitzi, D. B.; Dimitrakopoulos, C. D. Organic-Inorganic Hybrid Materials as Semiconducting Channels in Thin-Film Field-Effect Transistors. *Science* **1999**, *286*, 945−947.
(36) Chung, I.; Lee, B.; He, J.; Chang, R. P.; Kanatzidis, M. G. All-Solid-State Dye-Sensitized Solar Cells with High Efficiency. *Nature* **2012**, *485*, 486−489.
(37) Noel, N. K.; Stranks, S. D.; Abate, A.; Wehrenfennig, C.; Guarnera, S.; Haghighirad, A.-A.; Sadhanala, A.; Eperon, G. E.; Pathak, S. K.; Johnston, M. B.; et al. Lead-Free Organic-Inorganic Tin Halide Perovskites for Photovoltaic Applications. *Energy Environ. Sci.* **2014**, *7*, 3061−3068.
(38) Hao, F.; Stoumpos, C. C.; Cao, D. H.; Chang, R. P.; Kanatzidis, M. G. Lead-Free Solid-State Organic-Inorganic Halide Perovskite Solar Cells. *Nat. Photonics* **2014**, *8*, 489−494.
(39) Babayigit, A.; Thanh, D. D.; Ethirajan, A.; Manca, J.; Muller, M.; Boyen, H.-G.; Conings, B. Assessing the Toxicity of Pb- and Sn-Based Perovskite Solar Cells in Model Organism. *Sci. Rep.* **2016**, *6*, 18721.
(40) Filip, M. R.; Giustino, F. Computational Screening of Homovalent Lead Substitution in Organic-Inorganic Halide Perovskites. *J. Phys. Chem. C* **2016**, *120*, 166−173.
(41) Korbel, S.; Marques, M. A. L.; Botti, S. Stability and Electronic Properties of New Inorganic Perovskites from High-Throughput Ab Initio Calculations. *J. Mater. Chem. C* **2016**, *4*, 3157−3167.
(42) Lee, B.; Stoumpos, C. C.; Zhou, N.; Hao, F.; Malliakas, C.; Yeh, C.-Y.; Marks, T. J.; Kanatzidis, M. G.; Chang, R. P. H. Air-Stable Molecular Semiconducting Iodosalts for Solar Cell Applications: Cs_2SnI_6 as a Hole Conductor. *J. Am. Chem. Soc.* **2014**, *136*, 15379−15385.
(43) Maughan, A. E.; Ganose, A. M.; Bordelon, M. M.; Miller, E. M.; Scanlon, D. O.; Neilson, J. R. Defect Tolerance to Intolerance in the Vacancy-Ordered Double Perovskite Semiconductors Cs_2SnI_6 and Cs_2TeI_6. *J. Am. Chem. Soc.* **2016**, *138*, 8453−8464.
(44) Kaltzoglou, A.; Antoniadou, M.; Perganti, D.; Siranidi, E.; Raptis, V.; Trohidou, K.; Psycharis, V.; Kontos, A. G.; Falaras, P. Mixed-Halide $Cs_2SnI_3Br_3$ Perovskite as Low Resistance Hole-Transporting Material in Dye-Sensitized Solar Cells. *Electrochim. Acta* **2015**, *184*, 466−474.
(45) Kaltzoglou, A.; Antoniadou, M.; Kontos, A. G.; Stoumpos, C. C.; Perganti, D.; Siranidi, E.; Raptis, V.; Trohidou, K. N.; Psycharis, V.; Kanatzidis, M. G.; et al. Optical-Vibrational Properties of the Cs_2SnX_6 (X= Cl, Br, I) Defect Perovskites and Hole-Transport Efficiency in Dye-Sensitized Solar Cells. *J. Phys. Chem. C* **2016**, *120*, 11777−11785.
(46) Saparov, B.; Hong, F.; Sun, J.-P.; Duan, H.-S.; Meng, W.; Cameron, S.; Hill, I. G.; Yan, Y.; Mitzi, D. B. Thin-Film Preparation and Characterization of $Cs_3Sb_2I_9$: A Lead-Free Layered Perovskite Semiconductor. *Chem. Mater.* **2015**, *27*, 5622−5632.
(47) Park, B.-W.; Philippe, B.; Zhang, X.; Rensmo, H.; Boschloo, G.; Johansson, E. M. J. Bismuth Based Hybrid Perovskites $A_3Bi_2I_9$ (A: Methylammonium or Cesium) for Solar Cell Application. *Adv. Mater.* **2015**, *27*, 6806−6813.
(48) Hebig, J.-C.; Kühn, I.; Flohre, J.; Kirchartz, T. Optoelectronic Properties of $(CH_3NH_3)_3Sb_2I_9$ Thin Films for Photovoltaic Applications. *ACS Energy Lett.* **2016**, *1*, 309−314.
(49) Singh, T.; Kulkarni, A.; Ikegami, M.; Miyasaka, T. Effect of Electron Transporting Layer on Bismuth-Based Lead-Free Perovskite $(CH_3NH_3)_3Bi_2I_9$ for Photovoltaic Applications. *ACS Appl. Mater. Interfaces* **2016**, *8*, 14542−14547.
(50) Harikesh, P. C.; Mulmudi, H. K.; Ghosh, B.; Goh, T. W.; Teng, Y. T.; Thirumal, K.; Lockrey, M.; Weber, K.; Koh, T. M.; Li, S.; et al. Rb as an Alternative Cation for Templating Inorganic Lead-Free Perovskites for Solution Processed Photovoltaics. *Chem. Mater.* **2016**, *28*, 7496−7504.
(51) Kim, Y.; Yang, Z.; Jain, A.; Voznyy, O.; Kim, G.-H.; Liu, M.; Quan, L. N.; Garcíade Arquer, F. P.; Comin, R.; Fan, J. Z.; et al. Pure Cubic-Phase Hybrid Iodobismuthates $AgBi_2I_7$ for Thin-Film Photovoltaics. *Angew. Chem.* **2016**, *128*, 9738−9742.
(52) Xiao, Z.; Meng, W.; Mitzi, D. B.; Yan, Y. Crystal Structure of $AgBi_2I_7$ Thin Films. *J. Phys. Chem. Lett.* **2016**, *7*, 3903−3907.
(53) Fabian, D. M.; Ardo, S. Hybrid Organic-Inorganic Solar Cells Based on Bismuth Iodide and 1,6-Hexanediammonium Dication. *J. Mater. Chem. A* **2016**, *4*, 6837−6841.
(54) Slavney, A. H.; Hu, T.; Lindenberg, A. M.; Karunadasa, H. I. A Bismuth-Halide Double Perovskite with Long Carrier Recombination Lifetime for Photovoltaic Applications. *J. Am. Chem. Soc.* **2016**, *138*, 2138−2141.
(55) McClure, E. T.; Ball, M. R.; Windl, W.; Woodward, P. M. Cs_2AgBiX_6 (X = Br, Cl): New Visible Light Absorbing, Lead-Free Halide Perovskite Semiconductors. *Chem. Mater.* **2016**, *28*, 1348−1354.
(56) Volonakis, G.; Filip, M. R.; Haghighirad, A. A.; Sakai, N.; Wenger, B.; Snaith, H. J.; Giustino, F. Lead-Free Halide Double Perovskites via Heterovalent Substitution of Noble Metals. *J. Phys. Chem. Lett.* **2016**, *7*, 1254−1259.
(57) Wei, F.; Deng, Z.; Sun, S.; Xie, F.; Kieslich, G.; Evans, D. M.; Carpenter, M. A.; Bristowe, P.; Cheetham, T. The Synthesis, Structure and Electronic Properties of a Lead-Free Hybrid Inorganic-Organic Double Perovskite $(MA)_2KBiCl_6$ (MA = Methylammonium). *Mater. Horiz.* **2016**, *3*, 328−332.
(58) Filip, M. R.; Hillman, S.; Haghighirad, A. A.; Snaith, H. J.; Giustino, F. Band Gaps of the Lead-Free Halide Double Perovskites $Cs_2BiAgCl_6$ and $Cs_2BiAgBr_6$ from Theory and Experiment. *J. Phys. Chem. Lett.* **2016**, *7*, 2579−2585.
(59) Meyer, G.; Gaebell, H. Halo-Elpasolites. IV. On Bromo-Elpasolites $Cs_2B^IM^{III}Br_6$, B^I = Li, Na; M^{III} = Sc, Y, La−Lu, In, V, Cr). *Z. Naturforsch., B: J. Chem. Sci.* **1978**, *33*, 1476−1478.
(60) Baud, G.; Baraduc, L.; Gaille, P.; Cousseins, J. C. New Chloride Perovskites of the Type $Cs_2KB^{III}Cl_6$. *C. R. Seances Acad. Sci., Ser. C* **1971**, *272*, 1328−1331.
(61) Morss, L. R.; Siegal, M.; Stenger, L.; Edelstein, N. Preparation of Cubic Chloro Complex Compounds of Trivalent Metals: Cs_2NaMCl_6. *Inorg. Chem.* **1970**, *9*, 1771−1775.
(62) Meyer, G.; Linzmeier, P. Neue Chlor-Elpasolithe vom Typ $Cs_2AgLnCl_6$ (Ln = Sc, Y, Ce−Nd, Sm−Lu). *Rev. Chim. Miner.* **1977**, *14*, 52−57.

DOI: 10.1021/acsenergylett.6b00499
ACS Energy Lett. 2016, 1, 1233−1240

(63) Haegele, R.; Verscharen, W.; Babel, D. Einkristall-Strukturdaten Einiger Fluoride und Cyanide $A_2B^IM^{III}X_6$ der Elpasolithfamilie. *Z. Naturforsch., B: J. Chem. Sci.* **1975**, *30*, 462−465.
(64) Tressaud, A.; Khaïroun, S.; Chaminade, J. P.; Couzi, M. Structural Phase Transitions in $Rb_2KM^{III}F_6$ Elpasolites. I. Crystal Chemistry and Calorimetric Studies. *Phys. Status Solidi A* **1986**, *98*, 417−421.
(65) Grannec, J.; Yacoubi, A.; Tressaud, A.; Rabardel, L. Structural and Magnetic Properties of Ternary Silver Flourides with a Cryolite-Related Structure. *Solid State Commun.* **1988**, *68*, 363−367.
(66) Steward, E. G.; Rooksby, H. P. Transitions in Crystal Structure of Cryolite and Related Fluorides. *Acta Crystallogr.* **1953**, *6*, 49−52.
(67) Guengard, H.; Grannec, J.; Tressaud, A.; Flerov, I. N.; Gorev, M. V.; Melnikova, S. V. Ferroelastic Phase Transition in Elpasolite Tl_2KInF_6. *Phase Transitions* **1996**, *56*, 79−85.
(68) Ihringer, J.; Wu, G.; Hoppe, R.; Hewat, A. Phase Transitions and Structures in the Rare Earth Hexafluorides Cs_2NaHoF_6, Rb_2NaHoF_6, Cs_2KHoF_6 and Cs_2RbHoF_6 at $12 < T < 300$ K. *J. Phys. Chem. Solids* **1984**, *45*, 1195−1200.
(69) Tressaud, A.; Khaïroun, S.; Rabardel, L.; Kobayashi, T.; Matsuo, T.; Suga, H. Phase Transitions in Ammonium Hexafluorometallates-(III). *Phys. Status Solidi A* **1986**, *96*, 407−414.
(70) Bode, H.; Voss, E. Strukturen der Hexafluorometallate(III). *Z. Anorg. Allg. Chem.* **1957**, *290*, 1−16.
(71) Babel, D.; Haegele, R.; Pausewang, G.; Wall, F. Ueber Kubische und Hexagonale Elpasolithe $A^I_2B^IM^{III}F_6$. *Mater. Res. Bull.* **1973**, *8*, 1371−1382.
(72) Chadwick, B. M.; Jones, D. W.; Wilde, H. J.; Yerkess, J. X-ray and Neutron-Diffraction Studies of the Crystal Structures of the Dicesium Lithium Hexacyanometallates of Manganese(III) and Chromium(III). *J. Crystallogr. Spectrosc. Res.* **1988**, *18*, 55−66.
(73) Meyer, G. Halo-Elpasolites. VI. The First Iodo-Elpasolites $Cs_2B^IM^{III}I_6$ (B^I = Li, Na). *Z. Naturforsch., B: J. Chem. Sci.* **1980**, *35*, 394−396.
(74) Schneider, S.; Hoppe, R. Über Neue Verbindungen Cs_2NaMF_6 und K_2NaMF_6 Sowie Über Cs_2KMnF_6. *Z. Anorg. Allg. Chem.* **1970**, *376*, 268−276.
(75) Kojima, N. Gold Valence Transition and Phase Diagram in the Mixed-Valence Complexes $M_2[Au^IX_2][Au^{III}X_4]$;(M = Rb, Cs; X = Cl, Br, and I). *Bull. Chem. Soc. Jpn.* **2000**, *73*, 1445−1460.
(76) Biswas, K.; Du, M.-H. Energy Transport and Scintillation of Cerium-Doped Elpasolite Cs_2LiYCl_6: Hybrid Density Functional Calculations. *Phys. Rev. B: Condens. Matter Mater. Phys.* **2012**, *86*, 014102.
(77) Meyer, G. The Synthesis and Structures of Complex Rare-Earth Halides. *Prog. Solid State Chem.* **1982**, *14*, 141−219.
(78) Flerov, I. N.; Gorev, M. V.; Aleksandrov, K. S.; Tressaud, A.; Grannec, J.; Couzi, M. Phase Transitions in Elpasolites (Ordered Perovskites). *Mater. Sci. Eng., R* **1998**, *24*, 81−151.
(79) Goldschmidt, V. M. Die Gesetze der Krystallochemie. *Naturwissenschaften* **1926**, *14*, 477−485.
(80) Jain, A.; Shin, Y.; Persson, K. A. Computational Predictions of Energy Materials Using Density Functional Theory. *Nature Rev. Mater.* **2016**, *1*, 15004.

DOI: 10.1021/acsenergylett.6b00499
ACS Energy Lett. 2016, 1, 1233−1240